Simulating Castable Aluminum Alloy Microstructures with AlloyGAN Deep Learning Model

Biao Yin and Yangyang Fan

Abstract Material scientists have made progress in controlling alloy performance through microstructure quantification. However, attempts at numerically modeling microstructures have failed due to the complex nature of the solidification process. In this research, we present the AlloyGAN deep learning model to generate microstructures for castable aluminum alloys. This innovative model demonstrates its capacity to simulate the evolution of aluminum alloy microstructures in response to variations in composition and cooling rates. Specifically, it is successful to simulate various effects on castable aluminum, including: (1) the influence of Si and other elements on microstructures, (2) the relationship between cooling rate and Secondary Dendritic Arm Spacing, and (3) the impact of P/Sr elements on microstructures. Our model delivers results that match the accuracy and robustness of traditional computational materials science methods, yet significantly reduces computation time.

Keywords Deep learning · Aluminum alloys · Microstructure · Generative Adversarial Network

Introduction

The global metal market, crucial for industries like construction and aerospace, hinges on alloys for their reliable properties. With a projected worth of $18.5 trillion by 2030, alloy manufacturing is a key market driver [1]. Aluminum alloy casting and novel alloy development are crucial yet expensive, with a high rate of product rejections, which must be re-melted and re-cast due to various defects. Annually, the industry sees tens of millions of tons of metal casting products fall into this cycle

B. Yin
Data Science Program, Worcester Polytechnic Institute, Worcester, MA, USA
e-mail: byin@wpi.edu

Y. Fan (✉)
DeepAlloy, Portland, OR, USA
e-mail: yfan.deepalloy@gmail.com

The Minerals, Metals & Materials Society (ed.), *TMS 2024 153rd Annual Meeting & Exhibition Supplemental Proceedings*, The Minerals, Metals & Materials Series,
https://doi.org/10.1007/978-3-031-50349-8_69

[2]. Thus, efficient and reliable simulation models for accelerating scientific alloy discovery and reducing costs of manufacturing will bring immense economic and environmental benefits.

Traditional numerical methods have struggled with the complex solidification process in alloy formation, characterized by vast nonlinear chemical and physical interactions [3–7]. These models are intricate, computationally demanding, and require specific knowledge of material science, limiting their accessibility to the broader research community [8–13].

The problem thus is the urgent need for more efficient and accurate methods to generate microstructure images of metal alloys, based on initial conditions like chemical composition and manufacturing setting. Training from limited data, these methods should accurately model complicated chemical reactions while ensuring scientific validity and less computational complexity for practical application.

Deep learning techniques like VAEs, GANs, and Diffusions are being explored for microstructural analysis of materials in an early stage [14–18]. Their application remains limited, however, particularly in generating scientifically valid images based on basic alloy compositions. The existing deep learning methods haven't fully addressed the complexities inherent in material science [19–22]. This void emphasizes the need for innovative solutions capable of dealing with the complex nonlinear dynamics of the alloy microstructure formation and delivering robust generation capabilities to accelerate scientific alloy discovery.

To bridge this gap, we propose AlloyGAN, a ground-breaking approach leveraging the power of deep learning to create scientifically valid alloy microstructure images from basic alloy compositions (see Fig. 1). By integrating materials database, domain knowledge, and deep learning approach, AlloyGAN is thereby successfully simulating the microstructure of alloys with complex compositions and casting parameters. This innovative method seamlessly integrates materials databases, domain knowledge, and deep learning techniques, thereby enabling the accurate simulation of alloy microstructures with intricate compositions and casting parameters. The AlloyGAN model comprises three key components: a reliable materials database, a robust neural network, and domain expertise in materials science. By inputting alloy compositions and casting parameters, the model can produce corresponding microstructures. These generated micrographs closely resemble real-world microstructures, empowering materials engineers and scientists to assess material performance effectively.

Alloy Microstructure Database

Datasets play a crucial role in the training of deep learning models. Our dataset comprises 21,000 microstructure images, encompassing nine distinct alloys subjected to various manufacturing conditions, as detailed in Table 1. Each row within the table corresponds to a specific alloy type with unique chemical compositions. Furthermore, each alloy undergoes diverse cooling rates and modification

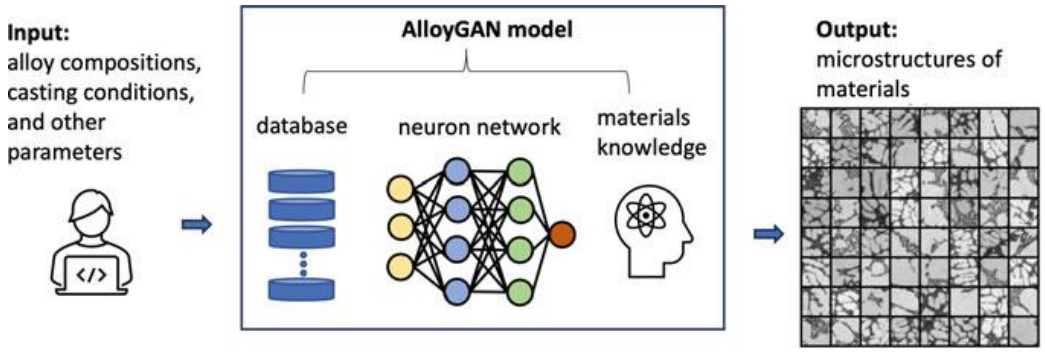

Fig. 1 Workflow of the AlloyGAN model. The model consists of three integral components: a materials database, a neural network, and materials knowledge. When alloy compositions and other relevant parameters are provided as input, the model proceeds to generate corresponding micrographs that closely mimic real-world microstructures

Table 1 Summary of the alloys employed in training the AlloyGAN deep learning model. It encompasses micrographs of nine distinct alloys, each subjected to varying cooling rates and modification conditions, all of which are integral to the training process

Alloy	Si	Fe	Cu	Mn	Mg	Ni	Cooling rate (K/s)	Modification
A356	7	0.5	0.25	0.35	0.3	0	2.5, 10, 57, 143	Yes, No
A360	9.5	0.6	0.1	0.05	0.5	0	2.5, 10, 57, 143	No
A369	11.5	1	0.5	0.25	0.4	0.05	2.5, 10, 57, 143	Yes, No
A339	12	1.2	2	0.5	1	1	2.5, 10, 57, 143	No
A393	22	1.3	0.9	0.1	1	2.3	2.5, 10, 57, 143	Yes, No
A355	5	0.65	1.25	0.55	0.5	0	2.5, 10, 57, 143	No
A308	5.5	0.8	4.5	0.5	0.1	0	2.5, 10, 57, 143	No
A319	6	1	4	0.4	0.55	0.35	2.5, 10, 57, 143	No
A332	9.5	0.9	3	0.5	2.1	0.5	2.5, 10, 57, 143	No

processes. These alloys were prepared using both sand and permanent mold techniques, resulting in cooling rates ranging from 1 to 100 K/s. Notably, alloys A356, A369, and A393 were modified by the addition of minute quantities of Strontium or Phosphorus (Sr/P), inducing significant alterations in the microstructures of these Si-based aluminum alloys through complex chemical reactions.

AlloyGAN Deep Learning Model

AlloyGAN builds upon the foundational principles of conditional Generative Adversarial Networks (cGANs) and incorporates unique adaptations that leverage prior knowledge of solidification reactions to generate scientifically valid alloy microstructure images. Similar to other Generative Adversarial Networks, AlloyGAN

comprises two major components: the Generative Network and the Discriminative Network. The role of the Generative Network is to produce synthetic microstructure images, while the Discriminative Network acts as a classifier, attempting to distinguish between real and generated data.

Through numerous training epochs, typically numbering in the hundreds or thousands, the Generative Network undergoes training loops to generate virtual micrographs that closely resemble real ones. Simultaneously, the Discriminative Network is trained to become progressively more proficient at discerning whether a given micrograph is genuine or generated ('fake'). The ultimate objective is for the Generative Network to produce micrographs so authentic that even experts would struggle to distinguish them from real ones. Meanwhile, the Discriminative Network should reach a point where it has a 50–50 chance of correctly identifying whether an image originates from the Generative Network.

Results and Discussion

As training epochs progress, these micrographs increasingly resemble real castable aluminum alloy structures. We assess the quality of the generated micrographs using three key metrics: (1) the model's capacity to accurately depict the influence of Si content on microstructures. (2) Its ability to demonstrate the relationship between Secondary Dendritic Arm Spacing and cooling rates. (3) Its effectiveness in revealing the effects of Sr/P modifications on microstructures.

Figure 2 displays representative micrographs of model-generated images featuring varying Si contents. In these images, white pixels represent Al phases, while black/gray pixels represent Si or Si compounds. As the Si content increases, the AlloyGAN model accurately depicts the rising presence of Si or Si compounds in the generated micrographs.

Figure 3 provides a quantitative representation of the increasing area fractions of Si phases in relation to Si content within the AlloyGAN-generated micrographs. These results serve as compelling evidence that the AlloyGAN model has effectively learned how Si contents influence aluminum microstructures.

The Secondary Dendritic Arm Spacing (SDAS) in the AlloyGAN-generated micrographs is assessed across various alloy compositions and cooling rates. It is a well-established fact that in the solidification process of metals, SDAS decreases with increasing cooling rates. This relationship can be quantified as follows [23]:

$$\lambda = k(CR)^{-n} (n > 0) \tag{1}$$

whereas λ represents SDAS, CR represents the cooling rate, k is a constant, and n is a positive number. We have measured the data for A356, A319, and A355 alloys, fitted it into Eq. 1, and plotted the results in Fig. 4. The outcomes demonstrate a strong fit to Eq. 1, indicating that the images generated by AlloyGAN align well with real-world

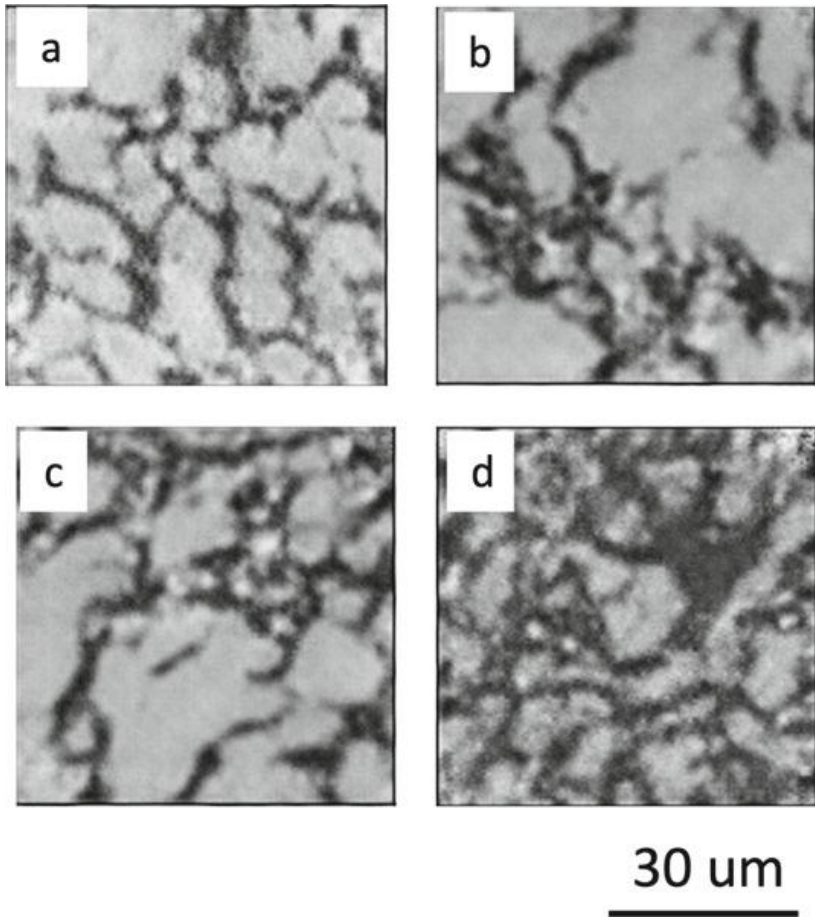

Fig. 2 AlloyGAN generated micrographs of A356, A332, A339, and A393 alloys which have Si contents of 7, 9.5, 12, and 22%, respectively. The black/gray pixels correspond to Si or Si compound phases

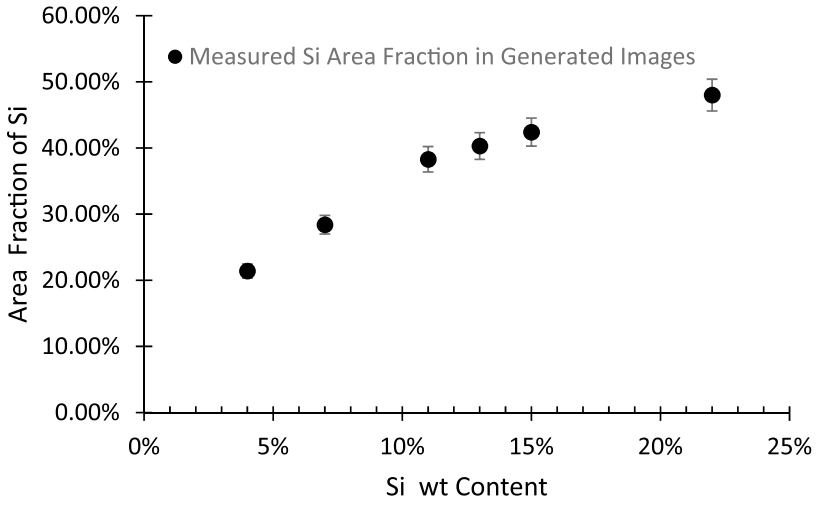

Fig. 3 Quantitative analysis of the relationship between Si contents and the area fractions of Si phases in AlloyGAN-generated micrographs

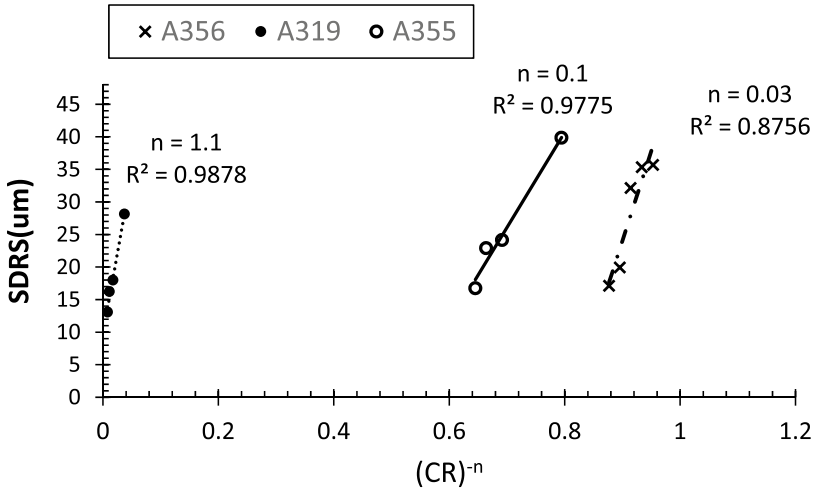

Fig. 4 Measurement of SDRS with cooling rate in AlloyGAN-generated micrographs

solidification phenomena. It underscores that the model has effectively captured how cooling rates influence SDAS in castable aluminum alloys.

Strontium and Phosphorus are frequently employed to modify the microstructure of castable aluminum alloys. The modified microstructures typically exhibit increased branching of eutectic Si phases, resulting in a smoother and more rounded appearance. This transformation occurs by enhancing twin density through a phenomenon known as impurity-induced twinning, as well as facilitating smoother eutectic growth during solidification [24].

In Fig. 5a–c, we observe AlloyGAN-generated micrographs of A356, A369, and A393 under unmodified conditions, while Fig. 5e, f display the corresponding generated images under modification conditions. These images distinctly reveal that the Si phases (depicted by dark pixels) are significantly finer and dispersed in the presence of Sr/P modifications. This evidence underscores that AlloyGAN has effectively learned how modification elements impact the microstructure of castable aluminum alloys.

AlloyGAN Website

We have made AlloyGAN accessible via a website (http://deepalloy.com). Users can create scientifically valid images given their text prompt to determining expected Alloy compositions within only 1 s. Enhancements of AlloyGAN to support different types of materials will continue to drive up its value to the material science community and customers.

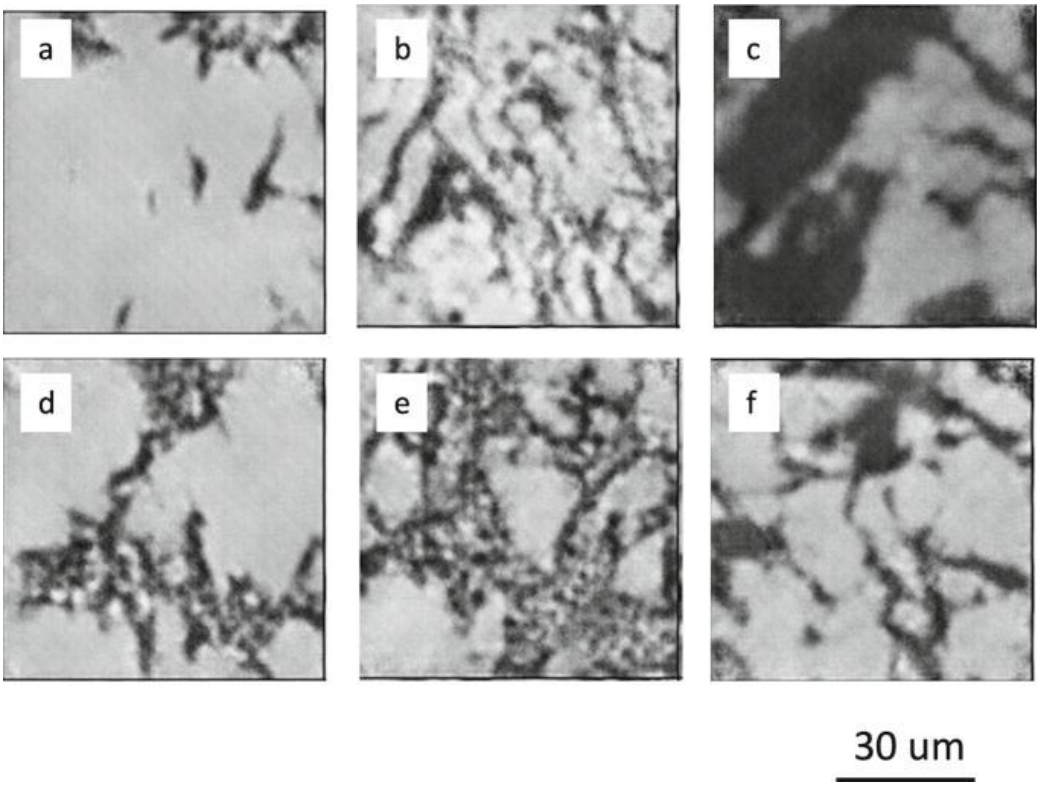

Fig. 5 **a–c** A356 alloy, A369, and A393 alloys with cooling rate = 2.5 K/s, unmodified. **d–f** A356 alloy, A369, and A393 alloys with cooling rate = 2.5 K/s, modified

Conclusion

AlloyGAN successfully generates microstructures of aluminum alloys under an array of promptable conditions, taking into account various chemical elements, manufacturing environments, as well as fundamental materials domain knowledge. AlloyGAN achieves results rivaling traditional computational material science methods in accuracy, while significantly reducing time and dependency on complex domain knowledge. With the launch of AlloyGAN, we unlock a path to remarkably efficient and ground-breaking applications in both material verification and scientific discovery in the field.

References

1. Allied Market Research (2022) Metal & metal manufactured products market 2021–2030. https://www.alliedmarketresearch.com. Accessed April 2022
2. Anderson MP, Grest GS, Srolovitz DJ (1985) Grain growth in three dimensions: a lattice model. Scr Metall (United States) 19(2)
3. Azimi SM, Britz D, Engstler M, Fritz M, Mücklich F (2018) Advanced steel microstructural classification by deep learning methods. Sci Rep 8(1):2128

4. Conti M, Di Pietro R, Mancini LV, Mei A (2009) Distributed data source verification in wireless sensor networks. Information Fusion 10(4):342–353
5. Eiken J (2009) Dendritic growth texture evolution in Mg-based alloys investigated by phase-field simulation. Int J Cast Met Res 22(1–4):86–89
6. Ferreira I, Ochoa L, Koeshidayatullah A (2022) On the generation of realistic synthetic petrographic datasets using a style-based GAN. Sci Rep 12(1):12845
7. Holm EA, Cohn R, Gao N, Kitahara AR, Matson TP, Lei B, Yarasi SR (2020) Overview: computer vision and machine learning for microstructural characterization and analysis. Metall and Mater Trans A 51:5985–5999
8. Iyer A, Dey B, Dasgupta A, Chen W, Chakraborty A (2019) A conditional generative model for predicting material microstructures from processing methods. arXiv preprint arXiv:1910.02133
9. Jung J, Na J, Park HK, Park JM, Kim G, Lee S, Kim HS (2021) Super-resolving material microstructure image via deep learning for microstructure characterization and mechanical behavior analysis. npj Comput Mater 7(1):96
10. Jung J, Yoon JI, Park HK, Jo H, Kim HS (2020) Microstructure design using machine learning generated low dimensional and continuous design space. Materialia 11:100690
11. Kim Y, Park HK, Jung J, Asghari-Rad P, Lee S, Kim JY, Kim HS (2021) Exploration of optimal microstructure and mechanical properties in continuous microstructure space using a variational autoencoder. Mater Des 202:109544
12. Kobayashi R (1993) Modeling and numerical simulations of dendritic crystal growth. Phys D 63(3–4):410–423
13. Lee JW, Goo NH, Park WB, Pyo M, Sohn KS (2021) Virtual microstructure design for steels using generative adversarial networks. Eng Rep 3(1):e12274
14. Lee KH, Yun GJ (2023) Microstructure reconstruction using diffusion-based generative models. Mech Adv Mater Struct 1–19
15. Li X, Zhang Y, Zhao H, Burkhart C, Brinson LC, Chen W (2018) A transfer learning approach for microstructure reconstruction and structure-property predictions. Sci Rep 8(1):13461
16. Li YL, Chen LQ (2006) Temperature-strain phase diagram for $BaTiO_3$ thin films. Appl Phys Lett 88(7)
17. Ma W, Kautz EJ, Baskaran A, Chowdhury A, Joshi V, Yener B, Lewis DJ (2020) Image-driven discriminative and generative machine learning algorithms for establishing microstructure–processing relationships. J Appl Phys 128(13)
18. Makhlouf ASH, Aliofkhazraei M (2015) Handbook of materials failure analysis with case studies from the aerospace and automotive industries. Butterworth-Heinemann
19. Moon IY, Lee HW, Kim SJ, Oh YS, Jung J, Kang SH (2021) Analysis of the region of interest according to CNN structure in hierarchical pattern surface inspection using CAM. Materials 14(9):2095
20. Na J, Kim G, Kang SH, Kim SJ, Lee S (2021) Deep learning-based discriminative refocusing of scanning electron microscopy images for materials science. Acta Mater 214:116987
21. Ning L, Cai Z, Liu Y, Wang W (2021) Conditional generative adversarial network driven approach for direct prediction of thermal stress based on two-phase material SEM images. Ceram Int 47(24):34115–34126
22. Oh S, Kim HK, Jeong TE, Kam DH, Ki H (2020) Deep-learning-based predictive architectures for self-piercing riveting process. IEEE Access 8:116254–116267
23. Fisher D, Kurz W (1998) Fundamentals of solidification. Fundam Solidi 1–316
24. Lu SZ, Hellawell A (1987) The mechanism of silicon modification in aluminum-silicon alloys: Impurity induced twinning. Metall Trans A 18:1721–1733